Water Supply

IWA PUBLISHING

Water Supply Vol 22 No 3, 2988 doi: 10.2166/ws.2021.422

Groundwater recharge pathway according to the environmental isotope: the case of Changwu area, Yangtze River Delta Region of China

Liang He[a,b,c,*], Junru Zhang[a,b,c], Suozhong Chen[a,b,c], Manqing Hou[a,b,c] and Junyi Chen[a,b,c]

[a] Key Laboratory of Virtual Geographic Environment, (Nanjing Normal University), Ministry of Education, Nanjing, Jiangsu 210023, China
[b] State Key Laboratory Cultivation Base of Geographical Environment Evolution (Jiangsu Province), Nanjing, Jiangsu 210023, China
[c] Jiangsu Center for Collaborative Innovation in Geographic Information Resource Development and Application, Nanjing, Jiangsu 210023, China
*Corresponding author. E-mail: heliang_nnu@163.com

ABSTRACT

Groundwater recharge is an important factor affecting water circulation. As groundwater has slow seepage, directly observing the seepage velocity and recharge path of groundwater in the aquifer is difficult. Environmental isotope technology has become an important means to clarify the mechanism of groundwater movement and the mechanism by which groundwater recharges from the micro and macro perspectives. The Changwu area of Jiangsu Province was taken as an example to identify the recharge sources of groundwater and the recharge paths of groundwater and surface water by using the measured data of isotopes D, ^{18}O, ^{34}S, and T. The results indicated that the shallow aquifer and the I confined aquifer in the Changwu area are mainly recharged by precipitation and surface lake water. The II confined aquifer along the Yangtze River is recharged by modern precipitation. Moreover, the II confined aquifer in the Henglin area was recharged by the ancient Yangtze River before 4,000 years ago, and no recharge relationship exists now. the recharge condition of the II confined aquifer around the northwest of Gehu Lake is in the climate environment of 8,000 years ago and was caused by the surface depression lake water at that time. Additionally, the concealed limestone aquifer is primarily supplied by the II confined aquifer, while the concealed sandstone aquifer supplies the II confined aquifer. Hence, to find out the recharge conditions of groundwater aquifers based on the environmental isotope is conducive to scientific and reasonable evaluation of groundwater resources and to ensure the sustainable development and utilization of groundwater resources.

Key words: Changwu area, confined aquifer, environmental isotopes, groundwater resources, recharge routes

HIGHLIGHTS

- Environmental isotope technology can elucidate the mechanism of groundwater movement and groundwater recharge.
- The isotopic concentration of groundwater generally reveals the weighted average of precipitation in the recharge area.
- The isotopic signatures preserved in the groundwater system are influenced by the geological setting and the hydrodynamic dispersion.

GRAPHICAL ABSTRACT

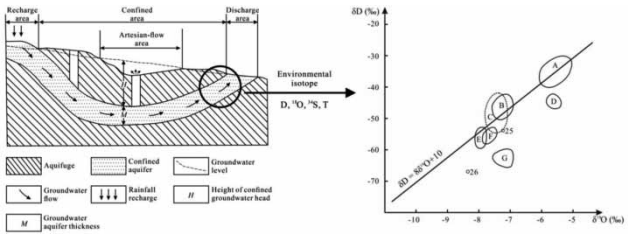

1. INTRODUCTION

Groundwater recharge refers to the process by which an aquifer or the water-bearing system obtains water from the outside world (Scanlon *et al.* 2002; Sophocleous 2002). Recharge sources are wide, including precipitation infiltration recharge, surface water, the condensate, the irrigation water return, the leakage, and the artificial recharge supply (Zhang *et al.* 2015;

Herrmann *et al.* 2016; Abe *et al.* 2018; Zhang & Wang 2020). According to the recharge sources of groundwater, Saether & Caritat (1997) defined three main recharge mechanisms that can coexist: direct recharge, indirect recharge, and local recharge (Liu *et al.* 2019). The recharge of groundwater by these three recharge mechanisms generally occurs in the form of infiltration of precipitation into the soil, which is a complex process of infiltration into the soil and infiltration through the soil matrix.

Ascertaining the recharge mechanism of groundwater is the foundation of the reasonable evaluation and scientific management of groundwater resources (Chatterjee *et al.* 2009; Dennehy *et al.* 2015). Since the mid-1980s, the international hydrogeological community has attached great importance to the quantitative study of groundwater recharge (Zektser 2002). The methods of quantitative research on groundwater recharge have gradually become more plentiful, and the application of methods has altered from one to a variety of technical methods. Currently, three types of techniques are applied to the study of groundwater recharge. The first is the physical method, such as the groundwater level dynamic method (Yu & Chu 2012), Darcy's law (Malekani *et al.* 2018), the zero flux surface method (Russoniello & Michael 2015), the baseflow partitioning method (Bartyzel & Rozanski 2016), and the permeameter method (Masoud *et al.* 2018; Pourghasemi *et al.* 2020). The second is the numerical simulation method, such as the water balance model (Yenehun *et al.* 2020) and the numerical model based on the Richards equation (Hassen *et al.* 2016; Hollander *et al.* 2016; Neto *et al.* 2016). Theoretically, the range of recharge amount estimated by a model is unlimited, but the reliability of a model is unverified by effective measured data. The third is the tracer method. Tracer technology is applied to the study of groundwater recharge and its theoretical method is developing rapidly. Three types of tracers are used in tracer technology: historical tracers (Boutton *et al.* 1999), environmental tracers (Li *et al.* 2017; Madrala *et al.* 2017), and artificial tracers (Clark *et al.* 2005; Moeck *et al.* 2017). Chloride and stable hydrogen and oxygen isotopes are the main environmental tracers, and the related research methods involve chlorine conservation methods (Leenheer *et al.* 2001) and the stable isotopes of the hydrogen and the oxygen method (Mezga *et al.* 2014; van Geldern *et al.* 2014; Vystavna *et al.* 2018). In the investigation of the groundwater recharge mechanisms, the stable hydrogen and oxygen isotopes are primarily employed to evaluate the recharge source and mechanism, and the conservation of the chlorine element can be utilized to calculate groundwater recharge.

The environmental isotopes most commonly used in groundwater studies include the stable isotopes deuterium (D), oxygen-18 (^{18}O), sulfur-34 (^{34}S), and the radioactive isotope tritium (T). Stable isotopes D and ^{18}O primarily reflect groundwater sources, hydraulic links, aquifer leakage, and paleoclimate changes (Kumar *et al.* 2019; Arumi *et al.* 2020; Kreis *et al.* 2020; Priestley *et al.* 2020). ^{34}S is chiefly employed to identify pollution sources and geothermal system water flow (Awad *et al.* 1995; Lee & Lee 2018). Radioactive isotope T is typically applied for the identification of recent recharges and the vadose transport process (Samborska *et al.* 2013). Comprehensive analysis of stable isotopes and radioisotopes can effectively reveal the transformed relationship between different water bodies.

Influenced by intensive exploitation, the groundwater level in the Changwu area, Jiangsu Province, has dropped dramatically, and the water circulation within the groundwater system has intensified (Ding *et al.* 2020). The hydraulic connection and recharge relationship between groundwater aquifers has become more complex, a development which generates difficulties in the evaluation of groundwater resources of each layer. To identify the recharge relationship of the groundwater and surface water in the study area under the current mining conditions, environmental isotopic D, ^{18}O, ^{34}S, and T data obtained in 2018 were used in this work. Through comprehensive comparative analysis, the recharge relationship of groundwater and surface water in each layer is determined. This approach provides a scientific basis for correctly delimiting the horizontal and vertical boundary types of different groundwater aquifers and improving the accuracy of groundwater resource evaluation in the study area.

2. MATERIALS AND METHODS

2.1. Study area

The study area comprises Changzhou City and the Wujin District of Jiangsu Province, located in the hinterland of the Yangtze River Delta. The terrain is flat, the surroundings and the expanse along the Taihu Lake area is slightly higher in the north and lower in the south, with an approximate elevation difference of 1–2 m. The study area covers an area of approximately 1,793 km^2, including the four municipal districts of Xinbei, Tianning, Zhonglou, and Wujin, which are called the 'Changwu area' (Hu *et al.* 2009). The geographical coordinates are 31°20–32°03′N and 119°40–120°12′E. The geographical location and hydrogeological profile of the study area are shown in Figure 1.

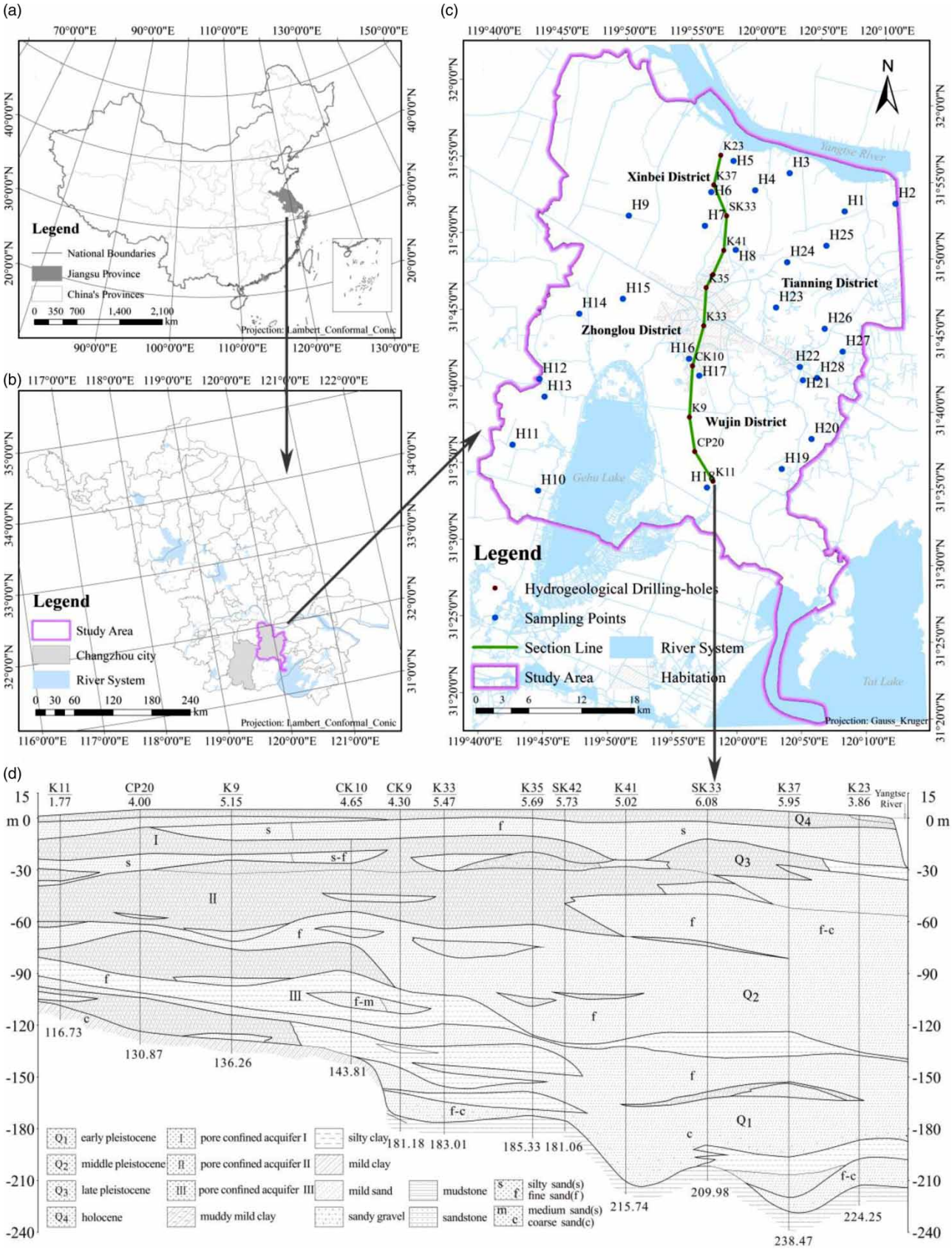

Figure 1 | Map of the study area and its geographical location. (a) Jiangsu Province, China, (b) Changzhou City, (c) spatial location of wells and sampling points in the study area, and (d) hydrogeological section.

Porous groundwater in the Changwu area is mainly stored in quaternary loose sediments. The porous phreatic water and the I, II, and III confined aquifers are distributed from top to bottom. Porous phreatic water and the I confined water are mainly supplied by atmospheric precipitation, surface water, and agricultural irrigation water and are chiefly discharged by exploitation and evaporation. The II and III confined aquifers are primarily employed for development and utilization, and the main mining layer of the groundwater is the II confined aquifer.

The II confined aquifer belongs to the Quaternary Middle Pleistocene aquifer, which is distributed in the Qidong formation and divided into the upper (II_1) and lower (II_2) aquifers. The II_2 aquifer is the most important aquifer, with extensive thickness and good water yield. From the mid-1980s to 2000, the II confined aquifer was in a long-term over-exploitation state, and the water level dropped dramatically, thereby forming a large-scale water level depression cone. As a result, the groundwater seepage field is seriously unbalanced and a series of environmental geological problems (such as land subsidence, ground fissures, and land collapse) was induced. This condition seriously threatens the safety of residents' lives and properties, destroys the ecological environment, and affects the sustainable development of the local economy. Accordingly, local governments at all levels have formulated several management regulations on groundwater mining restriction and prohibition since 2000. This endeavor curbed the continuous decline of the groundwater level, which has alleviated the rate of land subsidence. Ascertaining exploitable groundwater resources is the foundation of reasonable exploitation and the protection of the geological environment. This study delimits the boundary type of the groundwater flow numerical simulation area in view of the recharge relationship between the environmental isotopes in each layer of groundwater, surface water, and groundwater.

2.2. Sample collection

According to the isotopic characteristics of groundwater, the environmental isotopes of tritium (T), sulfur-34 (^{34}S), deuterium (D) and oxygen-18 (^{18}O) were selected to study the recharge relationship of groundwater in each layer of the Changwu area. A total of 28 samples was collected in March 2018. The hydrological and groundwater quality monitoring data in this paper are all derived from the groundwater environment monitoring reports of Wujin District, Changzhou City, Jiangsu Province, as well as the monitoring, series testing and test data of this study in recent years. Four samples from the I confined aquifer, 19 are from the II confined aquifer, one sample from the III confined aquifer, two samples from the limestone aquifer, and two samples from the sandstone aquifer. The spatial distribution of samples and the environmental isotope test data are shown in Figure 1 and Table 1, respectively. To compare the environmental isotopic contents of $\delta^{34}S$, δD, and $\delta^{18}O$ in the limestone water and the I confined aquifer, four limestone water samples were collected in the typical limestone area of Nanjing, and one of the I confined water samples was collected in the Suzhou area. The measured values of the environmental isotopes of the comparative samples are shown in Table 2.

2.3. Stable isotope characteristics

The content and correlation of the stable isotopes D, ^{18}O, and ^{34}S can qualitatively characterize the source and mechanism of groundwater recharge. Radioisotope T can be employed to identify the age of groundwater recharge and assess the renewal capacity of groundwater.

The values of δD and $\delta^{18}O$ in groundwater can indicate its recharge source, temperature during recharge, and hydrochemical process experienced by groundwater. There is a good linear relationship between δD and $\delta^{18}O$ in atmospheric precipitation (Ribeiro *et al.* 2020). Global meteoric water line $\delta D = 8\delta^{18}O + 10$. The degree of deviation of the δD and $\delta^{18}O$ values of groundwater from the local meteoric water line can be utilized to analyze the strength of the geophysical and chemical processes in the recharge and runoff processes of groundwater. The greater the deviation, the stronger the geochemical process (Ette *et al.* 2020).

2.4. Radioisotope characteristics

Tritium is a radioactive isotope of hydrogen and mainly exists in the environment in the form of HTO (Wigger & Van Loon 2018). Tritium is unstable and decays into helium with a half-life of 12.33 ± 0.33a. HTO molecules decay continuously in the natural water cycle, such that the tritium content in water lowers over time. Therefore, according to its decay law and the measured tritium content in groundwater, the recharge time and mixing mechanism of groundwater can be approximately estimated. The recovery methods of tritium concentration in precipitation are mainly related to the interpolation method, hyperbola method, unitary linear correlation method of different influencing factors, and factor analysis method (Grahek

Table 1 | Groundwater isotopic data in the Changwu area

Sampling points	Aquifer	Depth (m)	Test value of SO_4^{2-} (mmol/L)	Isotope test values			
				T (TU)	$\delta^{34}S$ (‰)	δD (‰)	$\delta^{18}O$ (‰)
H_1	II	74.84	0.15	6.59	38.9	−59	−7.8
H_2	II	70.72	0.03	8.71	27.8	−56	−8.1
H_3	II	71.67	0.03	3.85	–	−56	−7.9
H_4	II	72.11	0.02	11.12	–	−59	−7.9
H_5	II	65.90	0.02	4.98	–	−58	−7.8
H_6	II	73.22	0.03	2.69	–	−53	−7.8
H_7	I	25.58	0.12	8.76	10.1	−62	−7.4
H_8	II	59.17	0.29	12.29	5.1	−62	−7.0
H_9	II	71.19	0.02	10.72	42.7	−62	−7.6
H_{10}	II	40.12	0.05	7.50	24.6	−65	−7.0
H_{11}	II	45.40	0.05	6.61	–	−63	−7.1
H_{12}	II	50.83	0.27	6.65	28.3	−60	−7.0
H_{13}	I	29.15	0.27	12.36	19.7	−43	−5.7
H_{14}	II	55.93	0.57	5.44	22.6	−60	−7.2
H_{15}	III	128.88	1.05	4.86	26.4	−62	−7.4
H_{16}	I	20.09	1.54	23.57	10.4	−44	−5.8
H_{17}	II	60.52	0.63	4.42	15.2	−57	−7.3
H_{18}	II	47.71	0.03	8.39	16.1	−55	−7.1
H_{19}	I	22.8	0.23	7.95	20.5	−46	−5.4
H_{20}	II	60.44	0.56	4.65	20.4	−57	−7.9
H_{21}	Limestone	130.82	0.53	4.02	29.4	−57	−7.9
H_{22}	Limestone	140.43	0.31	2.77	30.0	−55	−7.7
H_{23}	II	61.02	0.02	3.90	–	−59	−7.5
H_{24}	II	60.05	0.33	12.90	14.9	−51	−6.9
H_{25}	Sandstone	200.64	0.11	9.09	14.1	−54	−7.3
H_{26}	Sandstone	183.89	1.00	2.25	27.6	−67	−8.3
H_{27}	II	57.70	0.30	1.57	43.4	−58	−7.8
H_{28}	II	59.14	0.54	1.83	33.8	−53	−7.6

'–' means not detected.

Table 2 | Environmental isotope measurement data of contrast samples

Sampling points	Aquifer	Area	Test value of SO_4^{2-} (mmol/L)	Isotope test values		
				$\delta^{34}S$ (‰)	δD (‰)	$\delta^{18}O$(‰)
N_1	Limestone	Nanjing	8.03	28.9	−43	−7.3
N_2	Limestone	Nanjing	5.25	30.6	−46	−7.7
N_3	Limestone	Nanjing	7.58	28.3	−48	−7.0
N_4	Limestone	Nanjing	12.47	26.4	−44	−7.3
S	I	Suzhou	0.31	16.2	−36	−5.3

et al. 2016; Kashiwaya *et al.* 2017; Larionova *et al.* 2017; Ansari *et al.* 2018; Vu *et al.* 2020). The tritium recovery curve of the atmospheric precipitation in the Nanjing area established by Zhang *et al.* (2011) is shown in Figure 2.

In 1963, the tritium concentration in the precipitation in the Nanjing area was as high as 1,764 TU, while that in the Nanjing area exceeded 200 TU between 1963 and 1968. By the 1970s, the tritium concentration in the precipitation of the Nanjing area was generally between 50 and 150 TU. After the 1980s, the level gradually returned to the natural one. According to the tritium recovery curve of the atmospheric precipitation in the Nanjing area, the average tritium concentration of groundwater formed by atmospheric precipitation in different periods can be recovered. The evolution path of tritium in groundwater can then be deduced on the basis of the tritium decay cycle.

3. RESULTS

3.1. The relationship between SO_4^{2-} - $\delta^{34}S$ and T - $\delta^{34}S$

The $\delta^{34}S$ values of H13 and H19 in the I confined water samples are approximately 20‰ and belong to precipitation recharge. Meanwhile, the $\delta^{34}S$ value of H16 is at 10 ‰, an amount which is affected by acid rain which, in turn, is consistent with the high SO_4^{2-} value.

The $\delta^{34}S$ concentrations of H21 and H22 in the limestone aquifer samples are approximately 30 ‰, are close to the 28‰ to 30 ‰ range of the typical limestone distribution areas in Nanjing. Analysis revealed a direct spatial contact relationship between the limestone aquifer and the II confined aquifer in the Changwu area. Additionally, the groundwater level of limestone is lower than that of the II confined aquifer which, in turn, recharges the limestone aquifer. Given the high SO_4^{2-} concentrations in the limestone water, the minerals are still dissolved after the II confined aquifer is recharged into the limestone, and the gypsum is mainly responsible for the increase in SO_4^{2-} concentration.

The $\delta^{34}S$ concentrations of H25 and H2 in the sandstone aquifer samples are 14.1 ‰ and 27.6 ‰, respectively. As H25 is located in the sandstone outcrop area and is affected by modern acid rain, the $\delta^{34}S$ concentration is approximately 14 ‰. However, H26 is located in the buried sandstone area and contacts limestone aquifer, thereby resulting in the $\delta^{34}S$ concentration of 27.6‰, a value which is very close to that of the limestone distribution area.

The II confined aquifer includes 19 samples. When $T \leq 3$ TU, two samples (H27 and H28) in this set of data belong to the reduction of SO_4^{2-} and lead to the increase in $\delta^{34}S$ concentration. When $T > 3$ TU, 13 samples with $\delta^{34}S$ concentrations are present. The spatial distribution of this group of samples revealed that the SO_4^{2-} concentration of H9 is 0.02 mmol/L, and the $\delta^{34}S$ concentration is 42.7‰. These outcomes can be summed up as the reduction in SO_4^{2-}, thereby resulting in the increase in $\delta^{34}S$ concentration. The other 12 samples can be divided into two groups: when 4 TU $< T <$ 6 TU, four samples (H14, H15, H17, and H20) showed no relationship between T and $\delta^{34}S$. When $T > 6$ TU, eight samples showed the trend of T and $\delta^{34}S$ in inverse proportion, as shown in Figure 3.

3.2. The relationship between T–$\delta^{18}O$ and T–δD

The $\delta^{18}O$ concentrations of the samples H13, H16, and H19 in the I confined aquifer are stable in the range −5.6 ‰ to −5.8 ‰, and the δD concentrations are in the range −43 ‰ to −46 ‰. Given that H26 belongs to concealed sandstone aquifer, in

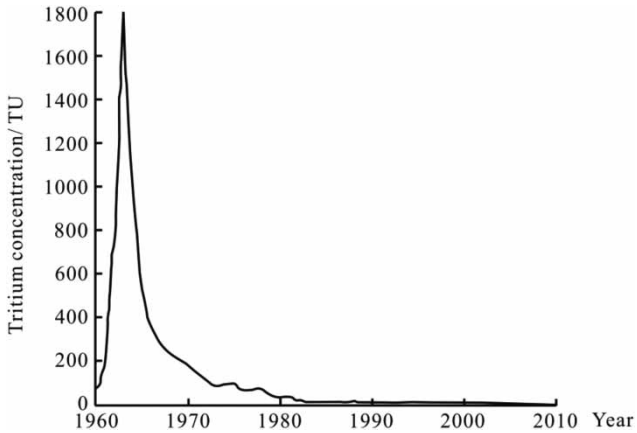

Figure 2 | Recovery curve of tritium concentration of atmospheric precipitation in Nanjing from 1960 to 2010.

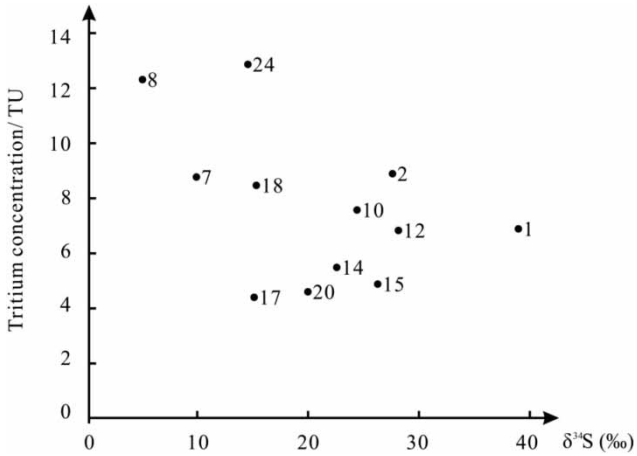

Figure 3 | The relationship between T–$\delta^{34}S$.

the H25 and H26 samples of the sandstone water body, the $\delta^{18}O$ concentration was −8.3‰ and the δD concentration was −67‰ (values which were lower than those of the other samples taken) because H26 belongs to the concealed sandstone aquifer. The relationships of the remaining samples T–$\delta^{18}O$ can be divided into the following two groups (Figure 4). One group of $\delta^{18}O$ concentrations is stable between −7.8‰ and −7.9‰, this generally does not change with the change of T concentrations, and includes H3, H4, H5, H6, H1, H20, and H21. The $\delta^{18}O$ concentrations of the other group of samples were between −6.8‰ and −7.8‰, and the distribution of $\delta^{18}O$ concentrations and T concentrations was approximately proportional.

The T–δD relationships for the remaining samples can be divided into the following two groups (Figure 5). One group of δD concentrations was stable between −60‰ and −65‰, and generally does not change with the change of T concentrations, and includes H7, H8, H9, H10, H11, H12, H14, and H15. The δD concentrations of the other group of samples were between −53‰ and −59‰. The δD concentrations and T concentrations were inversely proportional to each other.

3.3. The relationship between δD and $\delta^{18}O$

Figure 6 indicates that the H13, H16, and H19 samples of the I confined aquifer were relatively concentrated in the upper right corner and were located below the atmospheric water line $\delta D = 8\delta^{18}O + 10$. The H21 and H22 samples of the limestone

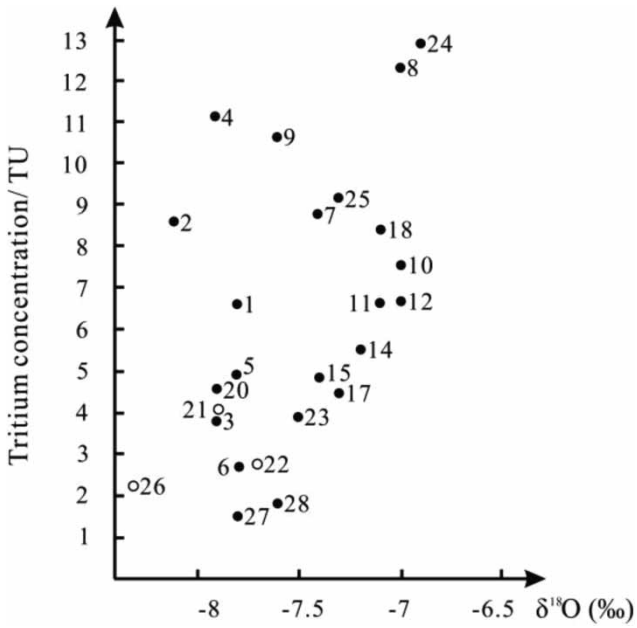

Figure 4 | The relationship between T–$\delta^{18}O$.

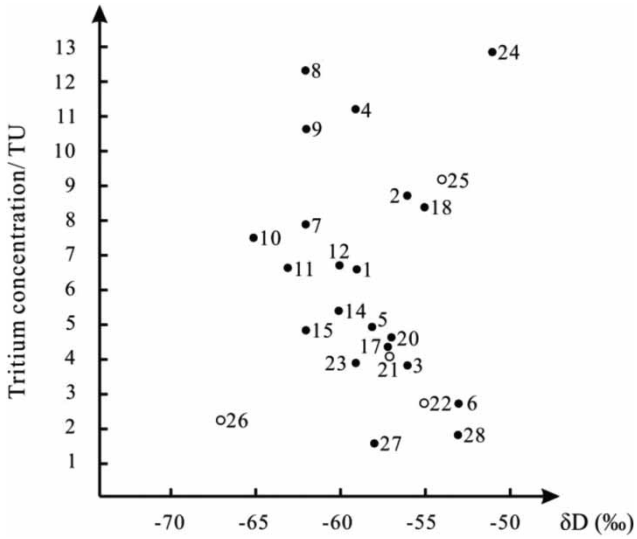

Figure 5 | The relationship between T–δD.

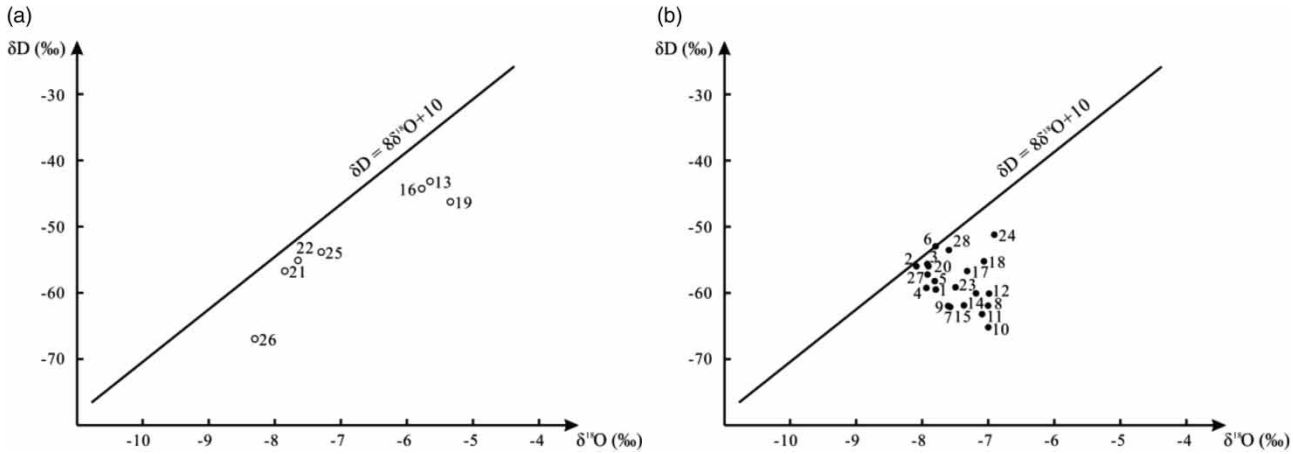

Figure 6 | The relationship between δD–δ^{18}O.

aquifer are relatively concentrated in the middle near the atmospheric water line. For the H25 and H26 samples from the sandstone aquifer, the H25 is close to the meteoric water line. This situation arises because H25 is located in the sandstone outcrop area, and the recharge environment of concealed sandstone aquifer and other samples vary, such as the disparity in the different average temperatures or times.

According to the geographical location and hydrogeological conditions of water samples, the II confined aquifer can be divided into the following three groups. The first group includes nine samples close to the meteoric water line, including H1, H2, H3, H4, H5, H6, H20, H27, and H28. The second group consists of eight samples, including H7, H8, H9, H10, H11, H12, H14, and H15. These samples are located under the meteoric water line and are distant from one another. The third group consists of four samples at the transition zone, including H17, H18, H23, and H24.

3.4. δD and δ^{18}O relation domain contrast

Figure 7 indicates that in the D domain of the I confined aquifer sample, the water has an evaporation effect and modern water recharge factors, thereby leading to the deviation from the atmospheric water line. The F domain of the II confined aquifer sample in the middle of the figure includes limestone aquifer samples H21 and H22 in the Henglin area. The limestone aquifer is proven to be recharged by the II confined aquifer because of the same distribution range observed. The E domain of the II confined aquifer samples include the six samples H1, H2, H3, H4, H5, and H6 from the area along the

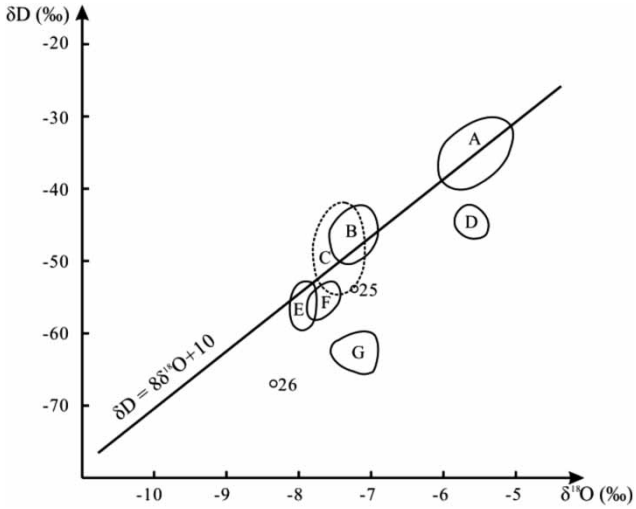

Figure 7 | $\delta D - \delta^{18}O$ relation domain contrast diagram.

Yangtze River. The relationship of the $T - \delta^{18}O$ group of this data proves that $\delta^{18}O$ does not change with the change of tritium concentration, so a recharge of the Yangtze River water occurs in terms of the recharge environment. Only the $T - \delta^{18}O$ mean value of the Yangtze River is relatively stable, and the tritium concentration can change with time. Thus, the water of the E domain has a recharge under the modern environment.

4. DISCUSSION

The D domain of the II confined water samples includes eight samples around the northwest of Gehu Lake where an evaporation effect occurs in the water, so it deviates far from the atmospheric water line. The biggest difference between the G samples and the E and F domain samples is that the water body of the G domain samples is evaporated and then recharged to groundwater. One of the samples in the E and F zones may be recharged by direct infiltration of precipitation, and the other may be recharged by infiltration of the Yangtze River water. Therefore, the G domain water body cannot receive the supply of the Yangtze River water, but only that of the lake water, because the lake water body is heated and evaporated. Regarding the location of the G domain, no evaporation of the lake water ensues under modern climate conditions and the lake water should be in a colder environment than that the modern climate. Therefore, no modern groundwater recharge happens in the G domain.

The water in the F domain is close to the atmospheric water line. Moreover, the lake water in this region is not recharged by the evaporation effect, a feature which may arise from natural precipitation or the Yangtze River water. However, compared with modern precipitation, Suzhou is located in the A domain, Nanjing is located in the B domain, Changwu should be located between them, and the I confined aquifer of Changwu is located in the D domain. If the effect of evaporation is subtracted, Changwu should be in the A domain or the B domain, which proves that the F domain cannot be the modern precipitation supply. Compared with the E domain which receives the water supply from the Yangtze River, the F domain is closer, but this relationship does not exist in the geographical location of the sample site. According to the ancient geographical location of the Changwu area, the present Henglin area is equivalent to the ancient Furong Lake low-lying land 2000 years ago (Zhao *et al.* 2007; Miao *et al.* 2016), and Furong Lake was connected to the Yangtze River in history. The predecessor of the Furong Lake is speculated to be a bend of the Yangtze River, that later degenerated into an ancient Furong Lake because the bend was gradually silted up. Historical research proves that the silting of the Yangtze River bend occurred four thousand years ago (Chen & Yang 1991; Min & Li 1992). Therefore, the water of the F domain is presumed to be recharged by the Yangtze River about four thousand years ago, and no recharge exists now.

With the development of the Holocene, the south bank of the Yangtze River (Changwu section) continuously deposited new sedimentary layers, and the river bank continued to move northward. Furthermore, a new aquifer was formed in the Weicun–Ligang–Shengang–Xiagang area along the river and received the recharge of the modern Yangtze River water.

5. CONCLUSIONS

A stable isotope reflects the change process of the climate and environment. At present, the commonly used comparison curve in the world is the ice core data of Greenland and Antarctica (Wunsch 2003; Landais *et al.* 2015) and includes the change and enrichment of the climate in the past 130,000 years, for which the climate in the past 8,000 years is relatively stable. According to environmental isotope, the recharge relationship of groundwater in the Changwu area is as follows: the shallow aquifer and the I confined aquifer are mainly recharged by atmospheric precipitation and surface lake water. The II confined aquifer along the Yangtze River is recharged by modern precipitation. The II confined aquifer in the Henglin area was recharged by the ancient Yangtze River before 4,000 years ago, and no recharge relationship exists now. The recharge condition of the II confined aquifer around the northwest of the Gehu Lake is in the climate environment of 8,000 years ago and was recharged by the surface depression lake water at that time.

The II confined aquifer in the transition zone of Gehu and the Henglin area does not have the recharge under the present climatic conditions and mainly accepts part of the leakage recharges from the I confined aquifer. Moreover, the concealed limestone aquifer is mainly supplied by the II confined aquifer, and the concealed sandstone aquifer supplies the II confined aquifer. The formation of the II confined aquifer in Changwu is directly related to the changes of the Yangtze River channel. The right channel of the Yangtze River erodes the south bank of the river. When the channel erodes to an aquifer at a certain depth, the groundwater in this aquifer drains into the Yangtze River, thereby causing vertical infiltration recharge of water above the aquifer.

AVAILABILITY OF DATA AND MATERIAL

The hydrological and groundwater quality monitoring data in this paper are all derived from the groundwater environment monitoring reports of Wujin District, Changzhou City, Jiangsu Province, as well as the monitoring, series testing and test data of this study in recent years. In total, 28 samples were collected in March 2018.

AUTHORS' CONTRIBUTIONS

Liang He: Conceptualization, Methodology, Validation. Junru Zhang: Data Curation, Writing – Original Draft. Suozhong Chen: Writing – Review & Editing, Funding acquisition. Manqing Hou: Resources, Visualization. Junyi Chen: Software, Supervision.

FUNDING

We are grateful for the funding support from the National Natural Science Foundation of China (Grant No. 41571386), the Priority Academic Program Development of Jiangsu Higher Education Institutions (Grant No. 1612206002), and the Postgraduate research and innovation plan project in Jiangsu Province (Grant No. KYCX21_1334).

DATA AVAILABILITY STATEMENT

All relevant data are included in the paper or its Supplementary Information.

REFERENCES

Abe, H., Tang, C., Takeuchi, N. & Kondoh, A. 2018 Influence of seasonal pumping on groundwater sources and flow system, Nagaoka Plain, Japan. *Groundwater* **56** (3), 470–481. doi:10.1111/gwat.12600.

Ansari, M. A., Mohokar, H. V., Deodhar, A., Jacob, N. & Sinha, U. K. 2018 Distribution of environmental tritium in rivers, groundwater, mine water and precipitation in Goa, India. *Journal of Environmental Radioactivity* **189**, 120–126. doi:10.1016/j.jenvrad.2018.04.004.

Arumi, J., Escudero, M., Aguirre, E., Salgado, J. C. & Aravena, R. 2020 Use of environmental isotopes to assess groundwater pollution caused by agricultural activities. *Isotopes in Environmental and Health Studies* **56** (5–6), 673–683. doi:10.1080/10256016.2020.1813124.

Awad, M. A., Nada, A. A., Hamza, M. S. & Froehlich, K. 1995 Chemical and isotopic investigation of groundwater in Tahta region, Sohag-Egypt. *Environmental Geochemistry and Health* **17** (3), 147–153. doi:10.1007/bf00126083.

Bartyzel, J. & Rozanski, K. 2016 Dating of young groundwater using four anthropogenic trace gases (SF6, SF5CF3, CFC-12 and Halon-1301): methodology and first results. *Isotopes in Environmental and Health Studies* **52** (4–5), 393–404. doi:10.1080/10256016.2015.1135137.

Boutton, T. W., Archer, S. R. & Midwood, A. J. 1999 Stable isotopes in ecosystem science: structure, function and dynamics of a subtropical Savanna. *Rapid Communications in Mass Spectrometry: RCM* **13** (13), 1263–1277. doi:10.1002/(sici)1097-0231(19990715)13:13 < 1263::aid-rcm653 > 3.0.co;2-j.

Chatterjee, R., Gupta, B. K., Mohiddin, S. K., Singh, P. N., Shekhar, S. & Purohit, R. 2009 Dynamic groundwater resources of National Capital Territory, Delhi: assessment, development and management options. *Environmental Earth Sciences* **59** (3), 669–686. doi:10.1007/s12665-009-0064-y.

Chen, Z. Y. & Yang, W. D. 1991 Quaternary paleogeography and paleoenvironment of Changjiang River estuarine region. *Acta Geographica Sinica* **04**, 459–466.

Clark, J. F., Hudson, G. B. & Avisar, D. 2005 Gas transport below artificial recharge ponds: insights from dissolved noble gases and a dual gas (SF6 and 3He) tracer experiment. *Environmental Science & Technology* **39** (11), 3939–3945. doi:10.1021/es049053x.

Dennehy, K. F., Reilly, T. E. & Cunningham, W. L. 2015 Groundwater availability in the United States: the value of quantitative regional assessments. *Hydrogeology Journal* **23** (8), 1629–1632. doi:10.1007/s10040-015-1307-5.

Ding, G., Chen, G., Liu, Y., Li, M. & Liu, X. 2020 Occurrence and risk assessment of fluoroquinolone antibiotics in reclaimed water and receiving groundwater with different replenishment pathways. *The Science of the Total Environment* **738**, 139802. doi:10.1016/j.scitotenv.2020.139802.

Ette, O. J., Igboro, B. S., Donatius, B., Okuofu, A. C., Madu, U. & Etteh, C. C. 2020 Environmental isotope characteristics of water sources in the Sokoto Basin – an evaluation of the role of meteoric recharge and residence time. *Isotopes in Environmental and Health studies* 1–12. doi:10.1080/10256016.2020.1822832.

Grahek, Z., Breznik, B., Stojkovic, I., Coha, I., Nikolov, J. & Todorovic, N. 2016 Measurement of tritium in the Sava and Danube Rivers. *Journal of Environmental Radioactivity* **162–163**, 56–67. doi:10.1016/j.jenvrad.2016.05.014.

Hassen, I., Hamzaoui-Azaza, F. & Bouhlila, R. 2016 Application of multivariate statistical analysis and hydrochemical and isotopic investigations for evaluation of groundwater quality and its suitability for drinking and agriculture purposes: case of Oum Ali-Thelepte aquifer, central Tunisia. *Environmental Monitoring and Assessment* **188** (3), 135. doi:10.1007/s10661-016-5124-7.

Herrmann, F., Baghdadi, N., Blaschek, M., Deidda, R., Duttmann, R., La Jeunesse, I., Sellami, H., Vereecken, H. & Wendland, F. 2016 Simulation of future groundwater recharge using a climate model ensemble and SAR-image based soil parameter distributions – A case study in an intensively-used Mediterranean catchment. *The Science of the Total Environment* **543** (Pt B), 889–905. doi:10.1016/j.scitotenv.2015.07.036.

Hollander, H. M., Wang, Z., Assefa, K. A. & Woodbury, A. D. 2016 Improved recharge estimation from portable, low-cost weather stations. *Groundwater* **54** (2), 243–254. doi:10.1111/gwat.12346.

Hu, J., Shi, B., Inyang, H. I., Chen, J. & Sui, Z. 2009 Patterns of subsidence in the lower Yangtze Delta of China: the case of the Suzhou-Wuxi-Changzhou region. *Environmental Monitoring and Assessment* **153** (1–4), 61–72. doi:10.1007/s10661-008-0336-0.

Kashiwaya, K., Muto, Y., Kubo, T., Ikawa, R., Nakaya, S., Koike, K. & Marui, A. 2017 Spatial variations of tritium concentrations in groundwater collected in the southern coastal region of Fukushima, Japan, after the nuclear accident. *Scientific Reports* **7** (1), 12578. doi:10.1038/s41598-017-12840-3.

Kreis, M., Taupin, J.-D., Patris, N. & Martins, E. S. P. R. 2020 Isotopic characterisation and dating of groundwater recharge mechanisms in crystalline fractured aquifers: example of the semi-arid Banabuiu watershed (Brazil). *Isotopes in Environmental and Health Studies* **56** (5–6), 418–430. doi:10.1080/10256016.2020.1797275.

Kumar, M., Ramanathan, A. L., Mukherjee, A., Sawlani, R. & Ranjan, S. 2019 Delineating sources of groundwater recharge and carbon in Holocene aquifers of the central Gangetic basin using stable isotopic signatures. *Isotopes in Environmental and Health Studies* **55** (3), 254–271. doi:10.1080/10256016.2019.1600515.

Landais, A., Masson-Delmotte, V., Stenni, B., Selmo, E., Roche, D. M., Jouzel, J., Lambert, F., Guillevic, M., Bazin, L. & Arzel, O. 2015 A review of the bipolar see-saw from synchronized and high resolution ice core water stable isotope records from Greenland and East Antarctica. *Quaternary Science Reviews* **114**, 18–32. doi:10.1016/j.quascirev.2015.01.031.

Larionova, N. V., Lukashenko, S. N., Lyakhova, O. N., Aidarkhanov, A. O., Subbotin, S. B. & Yankauskas, A. B. 2017 Plants as indicators of tritium concentration in ground water at the Semipalatinsk test site. *Journal of Environmental Radioactivity* **177**, 218–224. doi:10.1016/j.jenvrad.2017.06.032.

Lee, J.-H. & Lee, B.-J. 2018 Microbial reduction of Fe(III) and SO_4^{2-} and associated microbial communities in the alluvial aquifer groundwater and sediments. *Microbial Ecology* **76** (1), 182–191. doi:10.1007/s00248-017-1119-3.

Leenheer, J. A., Rostad, C. E., Barber, L. B., Schroeder, R. A., Anders, R. & Davisson, M. L. 2001 Nature and chlorine reactivity of organic constituents from reclaimed water in groundwater, Los Angeles County, California. *Environmental Science & Technology* **35** (19), 3869–3876. doi:10.1021/es001905f.

Li, Z., Chen, X., Liu, W. & Si, B. 2017 Determination of groundwater recharge mechanism in the deep loessial unsaturated zone by environmental tracers. *The Science of the Total Environment* **586**, 827–835. doi:10.1016/j.scitotenv.2017.02.061.

Liu, Z., Tan, H., Shi, D., Xu, P. & Elenga, H. I. 2019 Origin and formation mechanism of salty water in Zuli River catchment of the Yellow River. *Water Environment Research : A Research Publication of the Water Environment Federation* **91** (3), 222–238. doi:10.1002/wer.1040.

Madrala, M., Wasik, M. & Maloszewski, P. 2017 Interpretation of environmental tracer data for conceptual understanding of groundwater flow: an application for fractured aquifer systems in the Klodzko Basin, Sudetes, Poland. *Isotopes in Environmental and Health Studies* **53** (5), 466–483. doi:10.1080/10256016.2017.1330268.

Malekani, F., Ryan, M. C., Zebarth, B. J., Loo, S. E., Suchy, M. & Cey, E. E. 2018 A field-scale approach to estimate nitrate loading to groundwater. *Journal of Environmental Quality* **47** (4), 795–804. doi:10.2134/jeq2017.09.0369.

Masoud, M. H. Z., Basahi, J. M. & Zaidi, F. K. 2018 Assessment of artificial groundwater recharge potential through estimation of permeability values from infiltration and aquifer tests in unconsolidated alluvial formations in coastal areas. *Environmental Monitoring and Assessment* **191** (1), 31. doi:10.1007/s10661-018-7173-6.

Mezga, K., Urbanc, J. & Cerar, S. 2014 The isotope altitude effect reflected in groundwater: a case study from Slovenia. *Isotopes in Environmental and Health Studies* **50** (1), 33–51. doi:10.1080/10256016.2013.826213.

Miao, Q. Y., Zong, K. H., Chen, H. G. & Luo, D. 2016 Sedimentary division and characteristics of the Quaternary strata in the Yangtze River Delta (Jiangsu) region. *Shanghai Land & Resources* **37** (02), 51–56 + 64.

Min, Q. B. & Li, C. X. 1992 Late Quaternary paleogeography of the Yangtze River estuary. *Journal of Tongji University (Natural Science)* **04**, 459–466.

Moeck, C., Radny, D., Auckenthaler, A., Berg, M., Hollender, J. & Schirmer, M. 2017 Estimating the spatial distribution of artificial groundwater recharge using multiple tracers. *Isotopes in Environmental and Health Studies* **53** (5), 484–499. doi:10.1080/10256016.2017.1334651.

Neto, D. C., Chang, H. K. & van Genuchten, M. T. 2016 A mathematical view of water table fluctuations in a shallow aquifer in Brazil. *Groundwater* **54** (1), 82–91. doi:10.1111/gwat.12329.

Pourghasemi, H. R., Sadhasivam, N., Yousefi, S., Tavangar, S., Ghaffari Nazarlou, H. & Santosh, M. 2020 Using machine learning algorithms to map the groundwater recharge potential zones. *Journal of Environmental Management* **265**, 110525. doi:10.1016/j.jenvman.2020.110525.

Priestley, S. C., Meredith, K. T., Treble, P. C., Cendon, D. I., Griffiths, A. D., Hollins, S. E., Baker, A. & Pigois, J. P. 2020 A 35 ka record of groundwater recharge in south-west Australia using stable water isotopes. *The Science of the Total Environment* **717**, 135105. doi:10.1016/j.scitotenv.2019.135105.

Ribeiro, C., Velasquez, L. & Fleming, P. 2020 Origin of spring waters employing a multiparametric approach with special focus on stable isotopes 2H and 18O in the Lagoa Santa Karst region, Southern Brazil. *Isotopes in Environmental and Health Studies* **56** (2), 158–169. doi:10.1080/10256016.2020.1714608.

Russoniello, C. J. & Michael, H. A. 2015 Investigation of seepage meter measurements in steady flow and wave conditions. *Groundwater* **53** (6), 959–966. doi:10.1111/gwat.12302.

Saether, O. M. & Caritat, P. D. 1997 Geochemical processes, weathering, and groundwater recharge in catchments. A.A. Balkema, 416 pp.

Samborska, K., Rozkowski, A. & Maloszewski, P. 2013 Estimation of groundwater residence time using environmental radioisotopes (^{14}C,T) in carbonate aquifers, southern Poland. *Isotopes in Environmental and Health Studies* **49** (1), 73–97. doi:10.1080/10256016.2012.677041.

Scanlon, B. R., Healy, R. W. & Cook, P. G. 2002 Choosing appropriate techniques for quantifying groundwater recharge. *Hydrogeology Journal* **10** (1), 18–39. doi:10.1007/s10040-001-0176-2.

Sophocleous, M. 2002 Interactions between groundwater and surface water: the state of the science. *Hydrogeology Journal* **10** (1), 52–67. doi:10.1007/s10040-001-0170-8.

van Geldern, R., Baier, A., Subert, H. L., Kowol, S., Balk, L. & Barth, J. A. C. 2014 Pleistocene paleo-groundwater as a pristine fresh water resource in southern Germany–evidence from stable and radiogenic isotopes. *The Science of the Total Environment* **496**, 107–115. doi:10.1016/j.scitotenv.2014.07.011.

Vu, H., Merkel, B. J. & Weise, S. M. 2020 Origin of groundwater in Hanoi, Vietnam, revealed by environmental isotopes. *Isotopes in Environmental and Health Studies* **56** (4), 370–386. doi:10.1080/10256016.2020.1788548.

Vystavna, Y., Diadin, D. & Huneau, F. 2018 Defining a stable water isotope framework for isotope hydrology application in a large trans-boundary watershed (Russian Federation/Ukraine). *Isotopes in Environmental and Health Studies* **54** (2), 147–167. doi:10.1080/10256016.2017.1346635.

Wigger, C. & Van Loon, L. R. 2018 Effect of the pore water composition on the diffusive anion transport in argillaceous, low permeability sedimentary rocks. *Journal of Contaminant Hydrology* **213**, 40–48. doi:10.1016/j.jconhyd.2018.05.001.

Wunsch, C. 2003 Greenland–Antarctic phase relations and millennial time-scale climate fluctuations in the Greenland ice-cores. *Quaternary Science Reviews* **22** (15–17), 1631–1646. doi:10.1016/s0277-3791(03)00152-5.

Yenehun, A., Nigate, F., Belay, A. S., Desta, M. T., Van Camp, M. & Walraevens, K. 2020 Groundwater recharge and water table response to changing conditions for aquifers at different physiography: the case of a semi-humid river catchment, northwestern highlands of Ethiopia. *The Science of the Total Environment* **748**, 142243. doi:10.1016/j.scitotenv.2020.142243.

Yu, H.-L. & Chu, H.-J. 2012 Recharge signal identification based on groundwater level observations. *Environmental Monitoring and Assessment* **184** (10), 5971–5982. doi:10.1007/s10661-011-2394-y.

Zektser, I. S. 2002 Principles of regional assessment and mapping of natural groundwater resources. *Environmental Geology* **42** (2–3), 270–274. doi:10.1007/s00254-001-0496-5.

Zhang, Z. & Wang, W. 2020 Managing aquifer recharge with multi-source water to realize sustainable management of groundwater resources in Jinan, China. *Environmental Science and Pollution Research international* doi:10.1007/s11356-020-11353-3.

Zhang, W., Huan, Y., Yu, X., Liu, D. & Zhou, J. 2015 Multi-component transport and transformation in deep confined aquifer during groundwater artificial recharge. *Journal of Environmental Management* **152**, 109–119. doi:10.1016/j.jenvman.2015.01.027.

Zhang, Y. H., Ye, S. J. & Wu, J. C. 2011 A global model of recovering the annual mean tritium concentration in atmospheric precipitation. *Geological Review (Chinese Edition)* **57** (03), 409–418.

Zhao, B. C., Wang, Z. H. & Li, X. 2007 Characteristics and paleogeographic significance of paleo-incised valley sediments in southern Changjiang Delta Phain. *Journal of Palaeogeography (Chinese Edition)* **02**, 217–226.

First received 24 June 2021; accepted in revised form 23 November 2021. Available online 7 December 2021